DOI: 10.1002/asia.200800014

Hybridization-Sensitive On–Off DNA Probe: Application of the Exciton Coupling Effect to Effective Fluorescence Quenching

Shuji Ikeda and Akimitsu Okamoto*[a]

Abstract: The design of dyes that emit fluorescence only when they recognize the target molecule, that is, chemistry for the effective quenching of free dyes, must play a significant role in the development of the next generation of functional fluorescent dyes. On the basis of this concept, we designed a doubly fluorescence-labeled nucleoside. Two thiazole orange dyes were covalently linked to a single nucleotide in a DNA probe. An absorption band at approximately 480 nm appeared strongly when the probe was in a single-stranded state, whereas an absorption band at approximately 510 nm became predominant when the probe was hybridized with the complementary strand. The shift in the absorption bands shows the existence of an excitonic interaction caused by the formation of an H aggregate between dyes, and as a result, emission from the probe before hybridization was suppressed. Dissociation of aggregates by hybridization with the complementary strand resulted in the disruption of the excitonic interaction and strong emission from the hybrid. This clear change in fluorescence intensity that is dependent on hybridization is useful for visible gene analysis.

Keywords: absorption · aggregation · dyes · fluorescent probes · oligonucleotides

Introduction

Many fluorescent dyes have been developed for detection of a target biomolecule from amongst a range of candidates in extract mixtures, blotting analysis, and chromatographic fractions, to be used for observation of the functions of biomolecules in cells, such as detection of DNA, RNA, and proteins, and for measurement of membrane potentials.[1] These conventional fluorescent dyes always emit fluorescence when excitation light is shone on fluorescence-labeled samples. Therefore, dye molecules that do not take part in labeling of the target biomolecule have to be completely removed from the sample through several troublesome washing processes to extinguish the background fluorescence. Design of a "fluorescent dye" in which the fluorescence is turned off when the dye does not recognize the target biomolecule is very important for the establishment of bioimaging without the repetitive washing process, resulting in a highly reliable, labor-saving, and real-time-operating fluorescence observation. The chemistry of fluorescence quenching of dyes in the free state is a significant key for the design of the next generation of functional fluorescent dyes. So far, photophysics and photochemistry, such as excimer formation and dissociation,[2] photoinduced charge transfer,[3] photoinduced electron transfer,[4] and energy transfer between dyes,[5] have been applied to the molecular design of fluorescent probes that contain an "on–off" switching system.

In the design of on–off fluorescent DNA probes, the probes should show negligible emission for a single-stranded state and emit strongly upon binding with the target strand. Various DNA probes that give signals in a sequence-specific fashion, as exemplified by molecular beacons, have been widely used.[6] These probes have detected DNA sequences by using the change in the fluorescent intensity caused by the change in the distance between a fluorescent dye and a quencher dye that is linked at the strand ends by hybridization with the target sequence. However, many problems remain: 1) two types of dyes are required in a probe, thus they involve higher costs and difficult synthesis; 2) in most cases, both strand ends are occupied by dyes, thus biological applications such as PCR probes are limited; 3) probes require formation of higher-order structures such as a hairpin structure for efficient fluorescence quenching, thus they need sequences for structure formation, not for sequence

[a] Dr. S. Ikeda, Dr. A. Okamoto
Frontier Research System
RIKEN (The Institute of Physical and Chemical Research)
Wako, Saitama 351-0198 (Japan)
Fax: (+81) 48-467-9205
E-mail: aki-okamoto@riken.jp

Supporting information for this article is available on the WWW under http://www.chemasianj.org or from the author.

recognition; 4) each probe is labeled with one emission dye and multiple labeling is difficult because of the fluorescence-quenching mechanism; 5) the conformational degrees of freedom of dyes covalently linked to the strand ends strongly affect the quenching efficiency. Therefore, DNA probes that solve these problems need to be developed as the next generation of fluorescent probes.

Herein, we report a new concept for the design of fluorescent DNA probes. We used the fluorescence quenching by the exciton coupling effect of dyes to achieve turning off of fluorescence. The probe that we designed showed strong emission when it hybridized with the target strand, whereas the emission was suppressed strongly in the single-stranded state. This on–off probe overcomes the drawbacks suffered by conventional fluorescent probes.

Results and Discussion

Design of an Emission-Controlled Nucleoside

We focused on the photophysical behavior of the fluorescent dye thiazole orange. An important property of thiazole orange is the enhancement of fluorescence intensity upon intercalation with a DNA duplex; that is, this dye emits strong fluorescence in a DNA-binding state, whereas the fluorescence of the free dye is very weak.[7] The change in the fluorescence behavior of thiazole orange is due to the restriction of rotation around the methine bond between the two heterocyclic systems, and this increased rigidity as a result of the structural modifications prevents nonradiative deactivation.

The molecule produced by dimerization of thiazole orange is referred to as TOTO (Scheme 1a), which is used as a good DNA fluorescent stain.[8] Covalent linkage of two thiazole orange dyes through a biscationic linker to form a bichromophore increases the nucleic acid binding affinity. TOTO binds to DNA with a high DNA-binding ability through bis intercalation from the minor-groove side.[9]

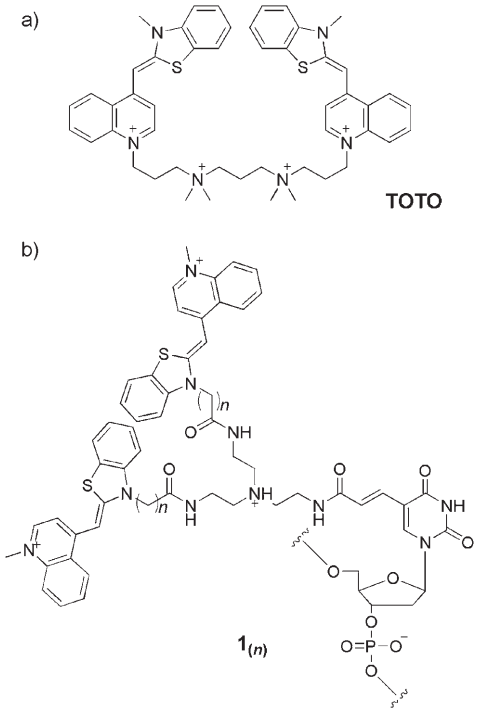

Scheme 1. Thiazole orange dimers: a) TOTO; b) newly synthesized fluorescent nucleotide, $\mathbf{1}_{(n)}$.

Much research on linking such a thiazole orange dye to an artificial DNA molecule or DNA analogue and its application to gene analysis has already been reported.[10,11] Indeed, these probes show strong fluorescence, but the quenching efficiency in the single-stranded state is often low. A demonstration of the use of a tethered thiazole orange dye for applications involving peptide nucleic acid (PNA) probe molecules has been reported previously.[12] Incorporation of thiazole orange into PNA somewhat improved the quenching efficiency in the single-stranded state, but the improvement is still small because the fundamental photophysical property of thiazole orange is scarcely controlled. In addition, the extraordinary costs in labor and money for synthesis of PNA labeled with thiazole orange are unavoidable. Although there are such problems, there is no doubt that thiazole orange is a very effective dye for DNA detection, as described above. A more precise design of fluorescent DNA based on characteristic photophysical properties of thiazole orange would give us more-sensitive DNA probes.

We designed a doubly fluorescence-labeled nucleoside (Scheme 1b). The dye is known to show little emission from the exciton coupling effect[13] when several fluorescent dyes arrange in parallel (H aggregation).[14] This effect is caused by a splitting of the excited state of dyes into two energy levels, and excitation to the upper energy level is followed by internal conversion to the lower energy level. The emis-

Abstract in Japanese:

遺伝子解析のための蛍光標識核酸プローブは、標的核酸に結合して点灯する機能、逆に言えば、標的と結合していないときには消灯する機能を持っているのが望ましい。そこで、蛍光色素チアゾールオレンジの会合体で観察されるエキシトン相互作用による自己蛍光消光を積極的に利用した新規蛍光性DNAプローブをデザインした。色素のインターカレーションや合成工程などを勘案して、チアゾールオレンジ2量体をウリジン5位に接続した人工ヌクレオシドが合成された。合成プローブが一本鎖状態でいるときの吸収バンドがハイブリダイゼーション後の吸収バンドに比べ短波長側に現れ、一本鎖状態での色素二量体による H 会合体の形成を示した。蛍光発光に関与する吸収が長波長側の吸収バンドだけであることを励起スペクトルが示しており、色素間のエキシトン相互作用による蛍光発光制御が働いていることが明確に示されている。その結果、蛍光発光は、ハイブリダイゼーション後に強く、一本鎖状態ではきわめて弱い。色素1個しか含まないプローブでは会合体形成が成立せず、一本鎖状態での蛍光消光の程度は小さい。標的 DNA 検出による新規「オン－オフ」DNA プローブの蛍光の変化は、目視でも容易に判別でき、ドットブロッティングのような遺伝子解析法を省力化する。

sion from the lower excitonic level is very weak because of the redistribution of the whole oscillator strength to the upper excitonic level transition. If two thiazole orange dyes were linked covalently to a DNA probe, the emission could be suppressed strongly in the single-stranded state by the exciton coupling effect. In contrast, strong emission would be observed when the probe binds to the target DNA because the aggregate is probably dissolved and each dye is expected to bind to the duplex structure. Therefore, design of probes showing the exciton coupling effect by the coupling of two fluorescent dyes is expected to produce a highly sensitive DNA probing system.

Based on this molecular-design concept, we designed a doubly fluorescence-labeled nucleoside as shown in Scheme 1b. Two thiazole orange dyes were linked to C5 of 2′-deoxyuridine because this is convenient for the intercalation of drugs from the major groove of DNA duplexes and a reduction in the synthetic steps. Additionally, on the basis of structural information reported earlier that quinoline rings locate at the minor-groove side and benzothiazole rings locate at the major groove in the DNA-binding structure of TOTO,[9] the nitrogen atom of the benzothiazole ring of thiazole orange was linked to a uracil base in a newly designed nucleoside.

Synthesis

The synthetic route is outlined in Scheme 2. The synthesis of a thiazole orange derivative $\mathbf{4}_{(n)}$ ($n=3$–6) was attained through a conventional dye synthetic protocol from a benzothiazole derivative with various lengths of carboxy linkers, $\mathbf{2}_{(n)}$.[15] To avoid damage to the dyes during the DNA synthetic process, we prepared a DNA strand containing a synthetic nucleoside with two amino linkers prior to the incorporation of carboxylate-activated dyes. A synthetic nucleoside with two amino linkers was prepared from a uridine derivative with an acrylate group at C5, **5**.[16] Two primary amino groups obtained by the coupling of **5** with tris(2-aminoethyl)amine were protected by trifluoroacetyl groups to give nucleoside **6**. Protection of the 5′-hydroxy group and the following phosphoramidation of the 3′-hydroxy group gave **7**, which was then incorporated into DNA strands through a conventional phosphoramidite method by using a DNA autosynthesizer. A DNA strand containing a doubly fluorescence-labeled nucleotide $\mathbf{1}_{(n)}$ was synthesized by mixing a diamino-modified DNA strand **8** with an activated dye $\mathbf{4}_{(n)}$. The short DNA strands (oligodeoxynucleotides; ODN) that were modified with dyes and their complementary strands that were prepared for the experiments described below are summarized in Table 1.

Photophysics of Fluorescent DNA

We measured absorption, excitation, and emission spectra of $\mathbf{1}_{(n)}$-containing ODNs with a variety of sequences and dye-linker lengths before and after hybridization with the complementary strands. The photophysical data and spectra of

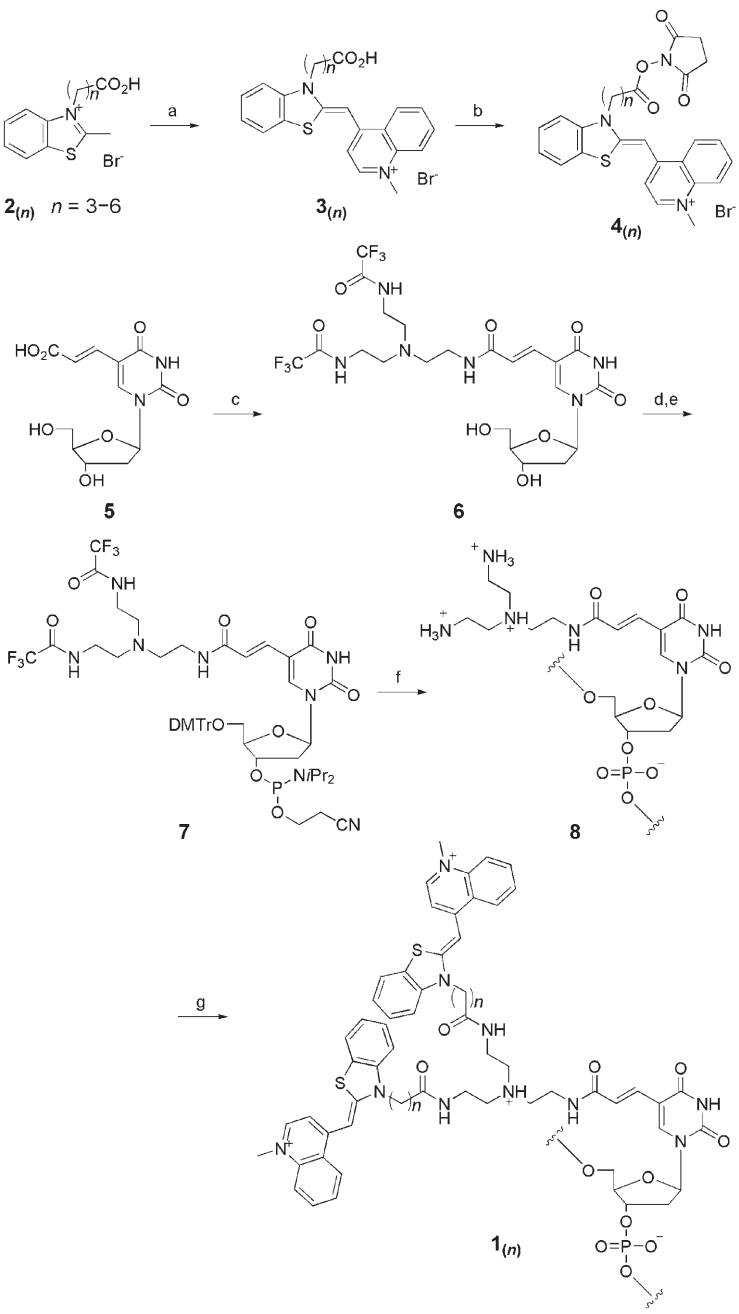

Scheme 2. Synthesis of artificial DNA containing the doubly dye-labeled nucleotide. Reagents and conditions: a) quinoline methiodide, triethylamine, dichloromethane, 25 °C, 16 h, 43 % ($n=3$), 28 % ($n=4$), 26 % ($n=5$), 22 % ($n=6$); b) *N*-hydroxysuccinimide, ethyl *N*,*N*-dimethylaminopropyl carbodiimide (EDCI), DMF, 25 °C, 16 h, no isolation; c) 1. *N*-hydroxysuccinimide, EDCI, DMF, 25 °C, 3 h, 2. tris(2-aminoethyl)amine, acetonitrile, 25 °C, 10 min, 3. ethyl trifluoroacetate, triethylamine, acetonitrile, 25 °C, 16 h, 37 %; d) 4,4′-dimethoxytrityl chloride, pyridine, 25 °C, 16 h, 80 %; e) 2-cyanoethyl *N*,*N*,*N*′,*N*′-tetraisopropylphosphordiamidite, 1*H*-tetrazole, acetonitrile, 25 °C, 2 h, quant.; f) DNA autosynthesizer with a standard phosphoramidite method, then 28 % aqueous ammonia, 55 °C, 4 h and then 25 °C, 16 h; g) $\mathbf{4}_{(n)}$, DMF, 100 mM sodium carbonate buffer solution (pH 9.0), 25 °C, 16 h. DMTr = 4,4′-dimethoxytrityl.

$\mathbf{1}_{(n)}$-containing ODN samples are summarized in Table 2 and Figure 1, respectively. Two absorption bands were observed

Table 1. Artificial DNA used in this study.

	Sequences (5′→3′)
ODN1	CGCAAT$\mathbf{1}_{(n)}$TAACGC
ODN1′	GCGTTAAATTGCG
ODN1″	GCGTTAGATTGCG
ODN2	TTTTTT$\mathbf{1}_{(4)}$TTTTTT
ODN2′	AAAAAAAAAAAAA
ODN3	TGAAGGGCTT$\mathbf{1}_{(4)}$TGAACTCTG
ODN3′	CAGAGTTCAAAAGCCCTTCA
ODN4	CGCAAT$\mathbf{9}_{(4)}$TAACGC
ODN5	CGCAAT$\mathbf{9}_{(4)}\mathbf{9}_{(4)}$AACGC
ODN(anti4.5S)	GCCTCCT$\mathbf{1}_{(4)}$CAGCAAATCC$\mathbf{1}_{(4)}$ACCGGCGTG
ODN(antiB1)	CCTCCCAAG$\mathbf{1}_{(4)}$GCTGGGAT$\mathbf{1}_{(4)}$AAAGGCGTG

Table 2. Photophysical properties of $\mathbf{1}_{(n)}$-incorporated DNA.[a]

	λ_{max} [nm] (ε [$cm^{-1}M^{-1}$])	λ_{em} [nm][b]	Φ_f[c]	I_{ds}/I_{ss}[d]	T_m [°C]
ODN1 ($n=3$)	480 (117000) 510 (93800)	537	0.096	–	–
ODN1 ($n=3$)/**ODN1′**	505 (145000)	529	0.298	7.6	66
ODN1 ($n=4$)	479 (156000) 509 (104000)	538	0.059	–	–
ODN1 ($n=4$)/**ODN1′**	509 (179000)	528	0.272	14.4	65
ODN1 ($n=5$)	480 (139000) 510 (107000)	538	0.043	–	–
ODN1 ($n=5$)/**ODN1′**	508 (172000)	529	0.208	8.1	67
ODN1 ($n=6$)	479 (139000) 509 (93300)	536	0.053	–	–
ODN1 ($n=6$)/**ODN1′**	509 (164000)	528	0.265	10.9	65
5′-CGCAATT-TAACGC-3′/**ODN1′**	–	–	–	–	58
ODN2	478 (221000) 505 (115000)	545	0.010	–	–
ODN2/**ODN2′**	513 (209000)	536	0.469	160	62
ODN3	482 (146000) 510 (145000)	535	0.074	–	–
ODN3/**ODN3′**	509 (191000)	530	0.232	4.5	74

[a] 2.5 μM DNA, 50 mM sodium phosphate buffer solution (pH 7.0), 100 mM sodium chloride. [b] Excited at 488 nm. [c] Excited at λ_{max} (longer wavelength when there are two λ_{max} values). [d] The ratio of the fluorescence intensities at the λ_{em} of duplex and single-stranded states.

at 400–550 nm for all the $\mathbf{1}_{(n)}$-containing ODN samples. An absorption band at shorter wavelength (ca. 480 nm) appeared more strongly when $\mathbf{1}_{(n)}$-containing ODN samples were in a single-stranded state, whereas an absorption band of longer wavelength (ca. 510 nm) became predominant when $\mathbf{1}_{(n)}$-containing ODN samples were hybridized with the complementary strands. The absorption band at approximately 510 nm is a typical band observed for a monomeric thiazole orange.[7]

The emission spectra were observed at ~530 nm as a single broad band. Hybridization of $\mathbf{1}_{(n)}$-containing ODN with the complementary strand is clearly distinguishable using the change in the emission intensity. The $\mathbf{1}_{(n)}$-containing ODN samples hybridized with the target DNA strands showed strong emission, whereas the emission intensity of the samples before hybridization was much weaker. In particular, the fluorescence of **ODN2**, which consists of a polypyrimidine sequence, was almost completely quenched in the single-stranded state. The ratio of emission intensities of duplex and single-stranded states (I_{ds}/I_{ss}) of **ODN2** at the wavelength of the emission maximum reached 160. A 20-mer ODN strand with a general sequence **ODN3** also showed a clear change in emission intensity before and after hybridization. The length of dye–uracil linkers may be important for fluorescence emission control. However, in the range of the linker length we investigated, the influence of the linker length on the I_{ds}/I_{ss} value of **ODN1** was very small, and the emission intensity clearly changed depending on the structural states of the ODN samples (Figure S1 in the Supporting Information).

The excitation spectra displayed a single broad peak at about 510 nm regardless of their structural states. This wavelength is in good agreement with the wavelength of one of the absorption bands. This indicates that the absorption participating in the fluorescence emission is only the band observed at approximately 510 nm and the absorption band at about 480 nm makes a negligible contribution to the emission.

Intramolecular Aggregation of Fluorescent Dyes

The non-emissive character observed in the single-stranded state is accepted as a general feature of the H aggregates of the dyes. Interaction between the dyes has been explained by Kasha in terms of the exciton coupling theory in which the excited state of the dye dimer splits into two energy levels (Figure 2).[17] On the basis of the exciton theory, the transition to the upper excitonic state is allowed for the H aggregates, which rapidly deactivate to the lower excitonic state. The excitonic coupling energy was estimated as 1230 cm^{-1} from the shift of the absorption band from 510 to 480 nm upon dimerization, which is similar to the energy reported for the coupling in H aggregates of cyanine dyes.[13e] Emission from the lower energy level is theoretically forbidden and thus the singlet excited state of the aggregate gets trapped in a non-emissive state.

To further investigate the mechanism of emission suppression of $\mathbf{1}_{(4)}$-containing ODN samples, we measured the absorption spectra of **ODN1** ($n=4$) under a variety of temperatures and concentrations. The change in sample temperature altered the ratio of the absorbance of two absorption bands (Figure 3a). With an increase in sample temperature, the absorption band at 479 nm decreased gradually and the band at 509 nm increased. At 487 nm, an isosbestic point is observed, showing the presence of two spectroscopic components. On the other hand, the change in concentration of **ODN1** ($n=4$) did not affect the ratio of absorbance of the two bands (Figure 3b). On increasing the sample concentration, an increase in absorbance of both absorption bands was observed. The plot of $\log(A_{479})$ versus $\log(A_{509})$, that is, the ratio of the logarithm of the absorbance of each band, was found to be linear (inset of Figure 3b), suggesting that the ratio of the two spectroscopic components was almost constant regardless of the concentration of ODN. These spectral changes indicate the formation of an intramolecular

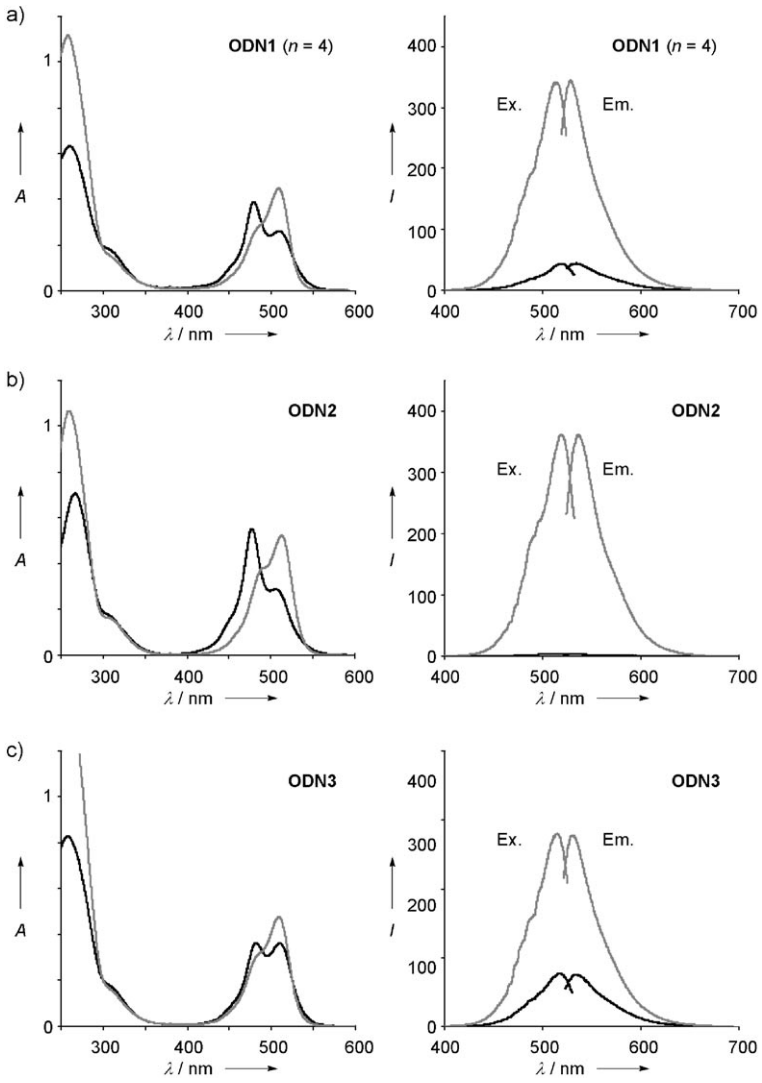

Figure 1. Absorption, excitation, and emission spectra of $\mathbf{1}_{(4)}$-containing ODNs. Absorption spectra are shown in the left-hand panels and excitation and emission spectra are shown in the right-hand panels. Spectra of $\mathbf{1}_{(4)}$-containing ODNs were measured in 50 mM sodium phosphate buffer solution (pH 7.0) containing 100 mM sodium chloride at 25 °C. Black trace: single-stranded ODN (ss); gray trace: ODN hybridized with the corresponding complementary DNA (ds). a) **ODN1** ($n=4$; 2.5 μM). Excitation spectra were measured for emission at a wavelength of 534 and 528 nm for ss and ds, respectively, and emission spectra were excited at 519 and 514 nm for ss and ds, respectively. b) **ODN2** (2.5 μM for the left-hand panel and 1 μM for the right-hand panel). Excitation spectra were measured for emission at a wavelength of 534 and 537 nm for ss and ds, respectively, and emission spectra were excited at 517 and 519 nm for ss and ds, respectively. c) **ODN3** (2.5 μM). Excitation spectra were measured for emission at a wavelength of 535 and 530 nm for ss and ds, respectively, and emission spectra were excited at 518 and 516 nm for ss and ds, respectively.

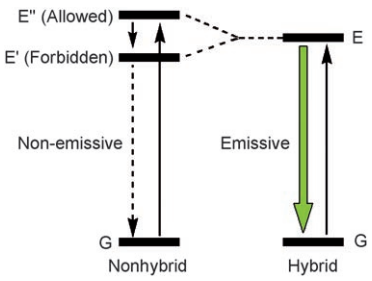

Figure 2. Schematic representation of the energy levels of the single- and double-stranded states of $\mathbf{1}_{(n)}$-containing ODN.

H aggregate by the bichromophoric system of ODN. Two conformational modes exist in a sample solution: an absorption band with a shorter wavelength (479 nm) is derived from a dimeric structure and one with longer wavelength (509 nm), which was enhanced with heating, is from monomeric dyes. A spectral band with the same wavelength as the absorption band with shorter wavelength was not observed in the excitation spectra, as shown in Figure 1, and this phenomenon is well explained on the basis of the exciton coupling theory shown in Figure 2.

Binding Mode of Dyes to Duplex

The duplex formed by $\mathbf{1}_{(4)}$-incorporated probes and their complementary strands was highly emissive and the structure was thermally stable. The melting temperature (T_m) of **ODN1** ($n=4$)/**ODN1′** increased 7–9 °C compared with a natural duplex 5′-CGCAATTTAACGC-3′/**ODN1′** (Table 2). The increase in the T_m values suggests that two cationic probe dyes effectively bind to duplexes formed with the target sequence. We also measured the CD spectrum of **ODN1** ($n=4$)/**ODN1′**. This duplex showed a broad negative signal and a sharp positive signal at 450–550 nm (Figure 4). These signals might result from mixed Cotton effects derived from different binding modes of dyes to DNA, which consist of a negative Cotton effect for dyes intercalating into a DNA duplex and a split-Cotton effect for dyes binding to the DNA groove.[18] The characteristic spectrum shape was also observed for the **ODN2**/**ODN2′** duplex (see Figure S2 in the Supporting Information). The results of T_m and CD measurements suggest that the dyes of $\mathbf{1}_{(4)}$ bind to the DNA duplex through intercalation and/or binding to the major groove and thermally stabilize the duplex structures. The binding of the dye to DNA strongly prevents the formation of a bichromophoric aggregate. As shown in Figure 1, an absorption band with longer wavelength derived from

CHEMISTRY
AN ASIAN JOURNAL

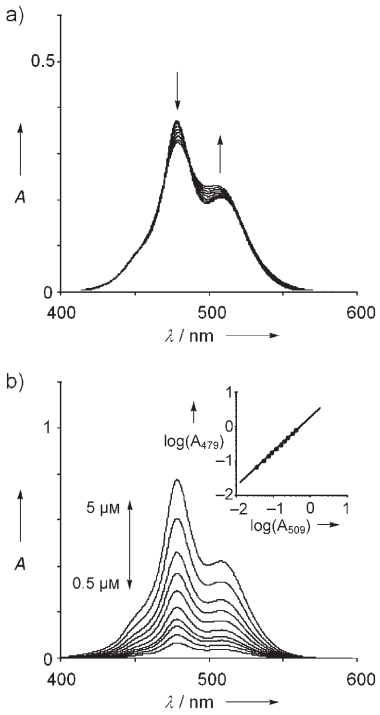

Figure 3. Effects of temperature and concentration on the absorption-band shape. Absorption spectra of **ODN1** ($n=4$) were measured in 50 mM sodium phosphate buffer solution (pH 7.0) containing 100 mM sodium chloride. a) Change in solution temperature. The ODN concentration was 2.5 μM. The spectra were recorded at 10 °C intervals between 10 and 90 °C. b) Change in solution concentration. The spectra were measured at 25 °C by using 0.5, 0.75, 1.0, 1.2, 1.5, 2.0, 2.5, 3.0, 4.0, and 5.0 μM of the ODN. Inset: plot of log(absorbance at 479 nm) against log(absorbance at 509 nm).

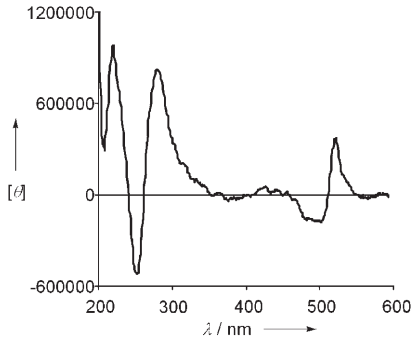

Figure 4. CD spectrum of **ODN1** ($n=4$)/**ODN1′**. CD spectra of the duplex (2.5 μM) were measured in 50 mM sodium phosphate buffer solution (pH 7.0) containing 100 mM sodium chloride at 25 °C. [θ] shown in [deg cm^2 dmol^{-1}].

monomeric dyes became predominant because of dissociation of the aggregates. Dissociation of the aggregates, that is, the disruption of the excitonic interaction, contributes to enhancement of the strong fluorescence emission.

To gain information on the effect of the base opposite the $\mathbf{1}_{(4)}$ base of **ODN1** ($n=4$) on fluorescence intensity, the fluorescence of the "mismatched" duplex with **ODN1″** (i.e., the strand containing a guanine base opposite $\mathbf{1}_{(4)}$) was measured (see Figure S3 in the Supporting Information). The fluorescence spectrum of the mismatched duplex showed a fluorescence signal at 529 nm that was weaker than that observed for "full-matched" **ODN1** ($n=4$)/**ODN1′**, but is still 5.8 times stronger than that for the single-stranded state. The small change in fluorescent intensity suggests that a decrease in DNA-binding ability of dyes caused by a mismatched base pair was not significant; the neighboring base pairs that are binding sites of dyes still remain in an ordered duplex structure even though the $\mathbf{1}_{(4)}$/G mismatched base pair partially disorders the duplex structure.

Photophysics of Singly Dye-Incorporated DNA

To verify the quenching ability of doubly dye-incorporated DNA, we prepared a singly dye-incorporated DNA molecule (Scheme 3). We synthesized a fluorescent ODN,

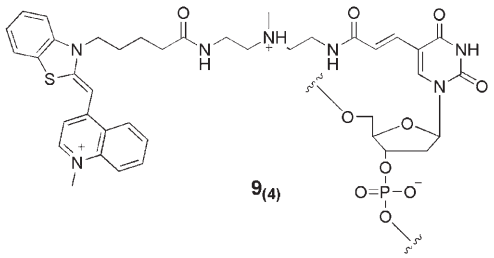

Scheme 3. Singly dye-incorporated DNA containing a nucleotide $\mathbf{9}_{(4)}$.

ODN4, which contains an artificial nucleotide modified with one thiazole orange dye, $\mathbf{9}_{(4)}$, (Table 1, and Scheme S1 in the Supporting Information), and measured its absorption and emission spectra. The absorption spectra of **ODN4** exhibited one absorption band at approximately 510 nm in both single-stranded and duplex states (Figure 5 and Table 3). Observation of no shift of the absorption band to shorter wavelength in the single-stranded state suggests that **ODN4** did not form a H aggregate. Because the exciton coupling effect does not work when a H aggregate is not formed, the fluorescence quenching in the single-stranded state is small, although there is still the structural control of fluorescence owing to the constrictive DNA environment.[19]

Although emission suppression in the single-stranded **ODN4** that contains a $\mathbf{9}_{(4)}$ nucleotide was small, the design of a $\mathbf{9}_{(4)}$-consecutive sequence, **ODN5**, recovered effective fluorescence quenching (Figure 6 and Table 4). The absorption spectra of **ODN5** showed a band shift to a shorter wavelength in the single-stranded state, which suggests that the dyes of two $\mathbf{9}_{(4)}$ nucleotides in **ODN5** formed an internucleotide H aggregate. This dimerization resulted in quenching of a single-stranded **ODN5** molecule, such as was observed for the $\mathbf{1}_{(n)}$-containing ODN. Formation of a H aggregate by the dyes of two $\mathbf{9}_{(4)}$ nucleotides in **ODN5** caused exciton coupling between dyes, which is responsible for efficient quenching of fluorescence emission. The DNA probe

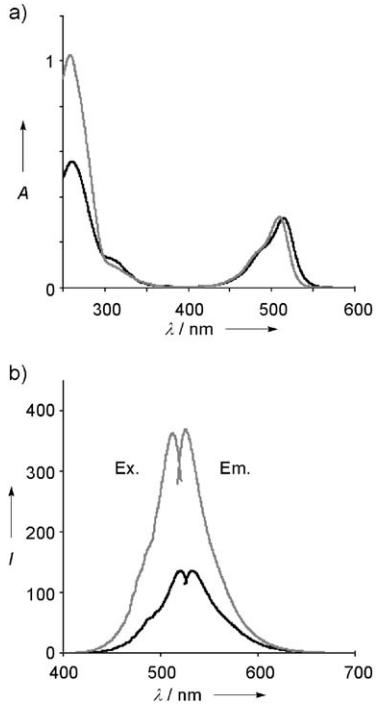

Figure 5. Absorption, excitation, and emission spectra of $\mathbf{9}_{(4)}$-containing ODN, **ODN4**. Spectra of **ODN4** (2.5 μM) were measured in 50 mM sodium phosphate buffer solution (pH 7.0) containing 100 mM sodium chloride at 25 °C. Black trace: single-stranded **ODN4** (ss); gray trace: **ODN4** hybridized with **ODN1′** (ds). a) Absorption spectra. b) Excitation and emission spectra. Excitation spectra were measured for emission at a wavelength of 532 and 526 nm for ss and ds, respectively, and emission spectra were excited at 520 and 512 nm for ss and ds, respectively.

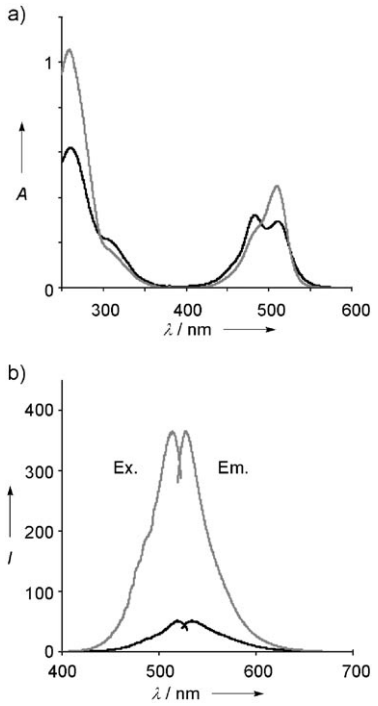

Figure 6. Absorption, excitation, and emission spectra of $\mathbf{9}_{(4)}$-containing ODN, **ODN5**. Spectra of **ODN5** (2.5 μM) were measured in 50 mM sodium phosphate buffer solution (pH 7.0) containing 100 mM sodium chloride at 25 °C. Black trace: single-stranded **ODN5** (ss); gray trace: **ODN5** hybridized with **ODN1′** (ds). a) Absorption spectra. b) Excitation and emission spectra. Excitation spectra were measured for emission at a wavelength of 534 and 514 nm for ss and ds, respectively, and emission spectra were excited at 528 and 519 nm for ss and ds, respectively.

Table 3. Photophysical properties of $\mathbf{9}_{(4)}$-incorporated DNA.[a]

	λ_{max} [nm] (ε [$cm^{-1}M^{-1}$])	λ_{em} [nm][b]	Φ_f[c]	I_{ds}/I_{ss}[d]	T_m [°C]
ODN4	515 (123000)	532	0.120	-	-
ODN4/ ODN1′	509 (125000)	526	0.307	3.4	65

[a] 2.5 μM DNA, 50 mM sodium phosphate buffer solution (pH 7.0), 100 mM sodium chloride. [b] Excited at 488 nm. [c] Excited at λ_{max} (longer wavelength when there are two λ_{max} values). [d] The ratio of the fluorescence intensities at the λ_{em} of duplex and single-stranded states.

Table 4. Photophysical properties of doubly $\mathbf{9}_{(4)}$-incorporated DNA.[a]

	λ_{max} [nm] (ε [$cm^{-1}M^{-1}$])	λ_{em} [nm][b]	Φ_f[c]	I_{ds}/I_{ss}[d]	T_m [°C]
ODN5	483 (123000) 511 (118000)	545	0.059	-	-
ODN5/ ODN1′	509 (180000)	528	0.275	10.3	71

[a] 2.5 μM DNA, 50 mM sodium phosphate buffer solution (pH 7.0), 100 mM sodium chloride. [b] Excited at 488 nm. [c] Excited at λ_{max} (longer wavelength when there are two λ_{max} values). [d] The ratio of the fluorescence intensities at the λ_{em} of duplex and single-stranded states.

containing a $\mathbf{9}_{(4)}$–$\mathbf{9}_{(4)}$ sequence might only be useful for the detection of the DNA containing an AA sequence.

DNA Detection

The fluorescence intensity of the $\mathbf{1}_{(n)}$-containing ODN was effectively alterable by the assistance of an excitonic interaction between the dyes tethered to a single nucleotide. This clear change in fluorescence that depends on hybridization with the target strand will be useful for quantitative and visible gene analysis. The fluorescence intensity of $\mathbf{1}_{(n)}$-containing ODN exhibited a linear relationship with the amount of the complementary DNA at a constant concentration of the ODN. As seen in Figure 7a, the fluorescent intensity of an **ODN1** ($n=4$)-containing solution increased in proportion to the amount of the added **ODN1′**, and reached a plateau when the **ODN1**/**ODN1′** ratio became 1:1. The $\mathbf{1}_{(4)}$-containing ODN allows determination of the existence of the hybridizable target strand with the naked eye. As shown in Figure 7b, hybridization of **ODN1** ($n=4$) with the complementary **ODN1'** resulted in emission of a light-green fluorescence upon irradiation with a 150-W halogen lamp. Emission from the hybrid was clearly distinguishable from a very weak fluorescence observed for nonhybridized **ODN1** ($n=4$).

Having established the fluorescence character of the new hybridization-sensitive probes, we tested the DNA analysis

CHEMISTRY
AN ASIAN JOURNAL

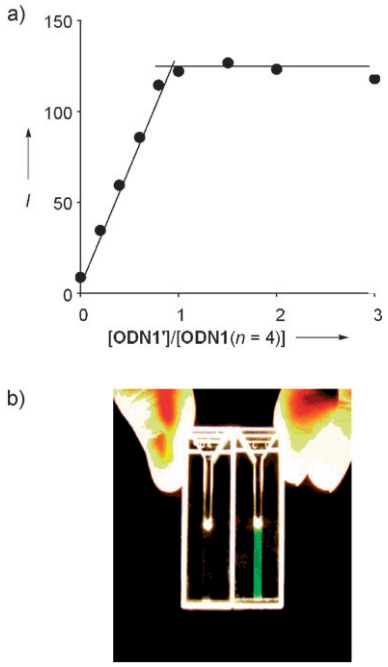

Figure 7. DNA detection. a) Linear relationship between the amount of **ODN 1′** and the fluorescence intensity of **ODN 1** ($n=4$). The fluorescent intensity of **ODN 1** (1.0 μM) at 529 nm was measured in a solution of 50 mM sodium phosphate buffer solution (pH 7.0) and 100 mM sodium chloride containing 0, 0.2, 0.4, 0.6, 0.8, 1.0, 1.5, 2.0, and 3.0 μM of **ODN 1′** at 25 °C. b) Fluorescence emission in cuvettes. The fluorescence from a solution containing 2.5 μM **ODN 1** ($n=4$) (left) or **ODN 1** ($n=4$)/**ODN 1′** (right) was measured in 50 mM sodium phosphate buffer solution (pH 7.0) containing 100 mM sodium chloride upon irradiation with a 150-W halogen lamp.

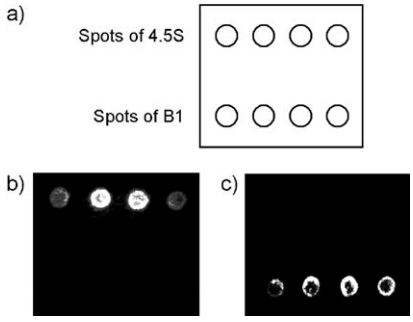

Figure 8. Dot blotting of DNA. a) Illustration of a nylon membrane in which different DNA sequences were applied. The four upper spots are for 4.5S RNA sequence-containing DNA, and the four lower spots are for B1 RNA sequence-containing DNA. b) Fluorescence emission from the membrane after incubation in a solution containing **ODN (anti4.5S)**. c) Fluorescence emission from the membrane after incubation in a solution containing **ODN (antiB1)**.

by means of dot blotting with the new probes. The target DNA sequences were the short DNA fragments that contained a B1 RNA sequence, which is one of the short interspersed nuclear elements in rodent genomes,[20] and the short DNA fragment containing a 4.5S RNA sequence, which is one of the small nuclear RNA molecules isolated from rodent cells and has extensive homology to the B1 family.[21] We prepared blotting probes **ODN (antiB1)** and **ODN (anti4.5S)** in which two $\mathbf{1}_{(4)}$ nucleotides were incorporated for higher fluorescence intensity and higher sensitivity. Multiple incorporation of $\mathbf{1}_{(4)}$ into a single probe is one of the valuable merits of our probes that is different from single fluorescence labeling of a conventional on–off probe, such as a molecular beacon. A nylon membrane sheet in which the denatured DNA fragments were spotted was incubated in a solution of the probe, **ODN (anti4.5S)** or **ODN (antiB1)**. The fluorescence of the blot spots was immediately readable at room temperature with a fluorescence-imaging instrument without repetitive washing processes after the blotting assay (Figure 8). As a result of incubation with the new probes, a strong emission from the spots of a 4.5S sequence was obtained for the addition of **ODN (anti4.5S)**, whereas the emission from the spots of a B1 sequence was negligible. In contrast, the addition of **ODN (antiB1)** showed a strong fluorescence signal for the spots of a B1 sequence, whereas a very weak fluorescence was observed for the spots of a 4.5S sequence. Our probes did not require numerous washing processes or antibody and enzyme-treating processes after blotting, which is quite different from the conventional blotting assays.

Conclusions

In conclusion, we designed conceptually new on–off fluorescent DNA probes. We used fluorescence quenching by the exciton coupling effect of thiazole orange dyes. Aggregation of two dyes tethered to a single nucleotide in DNA dramatically changes the photophysical properties of the dyes, as demonstrated by the large spectral shifts relative to the absorption of the monomeric dyes binding to DNA. Although the fluorescent intensity of our probes was effectively alterable by control of an excitonic interaction between the tethered dyes, it is still unavoidable that the quenching ability changes to some degree depending on the probe sequence, as seen in Figure 1. However, the present approach with an excitonic interaction exhibits a quenching ability that is high enough to work as an on–off probe, and also includes many advantages that are quite different from conventional assays: 1) the same two dyes covalently bind to one nucleotide, thus permitting lower costs and easy synthesis; 2) the strand ends do not need to be occupied by dyes, thus application to biological studies, such as the primers of PCR and the capture probes of DNA chips, may be unlimited; 3) it is not necessary to prepare any sequences for a higher-order structure formation to control fluorescence intensity, thus all of the probe sequence can be used for sequence recognition; 4) any thymines in a sequence can be replaced by the labeled nucleotides, thus multiple labeling of a strand is easy from the point of view of probe synthesis and effective for enhancement of fluorescence intensity, as in the experiment with **ODN (anti4.5S)** and **ODN (antiB1)**; 5) mobility of dyes covalently linked to one nucleotide is restricted, thus fluorescence quenching is effectively controlled. Design of such

an on–off fluorescent nucleotide is very important for the establishment of bioimaging assays without repetitive washing processes. The photophysical property exhibited by exciton-controlling probes is not only unique, but also applicable to the design of new fluorescent DNA probes for DNA sequencing, genotyping, monitoring of DNA structural transitions, and observation of gene expression.

Experimental Section

Materials and Methods

^{1}H, ^{13}C, and ^{31}P NMR spectra were measured with a JEOL JNM-α400. Coupling constants (J value) are reported in hertz. The chemical shifts are shown in ppm with residual dimethyl sulfoxide ($\delta = 2.48$ in ^{1}H NMR, $\delta = 39.5$ in ^{13}C NMR) and methanol ($\delta = 3.30$ in ^{1}H NMR, $\delta = 49.0$ in ^{13}C NMR) as internal standards. An external H_3PO_4 standard ($\delta =$ 0.00 ppm) was used for ^{31}P NMR measurements. ESI mass spectra were recorded on a Bruker Daltonics APEC-II. Reversed-phase HPLC was performed on CHEMCOBOND 5-ODS-H columns (10×150 mm^2) with a Gilson Chromatograph, Model 305 by using a UV detector, Model 118, at 260 nm. UV and fluorescence spectra were recorded on a Shimadzu UV-2550 spectrophotometer and RF-5300PC spectrofluorophotometer, respectively.

Syntheses

2$_{(4)}$: 2-Methylbenzothiazole (11.7 mL, 92 mmol) and 5-bromovaleric acid (13.7 g, 76 mmol) were mixed and stirred at 150 °C for 1 h. Methanol (50 mL) and then diethyl ether (200 mL) were added to the reaction mixture. The precipitate was filtered and washed with diethyl ether. The residue was dried under reduced pressure to give a light-purple powder (19.2 g). As the powder was a mixture of **2$_{(4)}$** and 2-methylbenzothiazolium bromide, the yield of **2$_{(4)}$** was calculated from the ratio of the areas of the proton peaks at 8.5 and 8.0 ppm of the ^{1}H NMR spectrum of the mixture in [D$_6$]DMSO, which were derived from **2$_{(4)}$** and 2-methylbenzothiazolium bromide, respectively. The yield of **2$_{(4)}$** was estimated as 9.82 g (14 mmol, 32 %). This mixture was used for the next reaction without further purification.

2$_{(3)}$: The compound was synthesized according to the synthetic protocol of **2$_{(4)}$**. The yield of **2$_{(3)}$** was 4 %.

2$_{(5)}$: The compound was synthesized according to the synthetic protocol of **2$_{(4)}$**. The yield of **2$_{(5)}$** was 35 %.

2$_{(6)}$: The compound was synthesized according to the synthetic protocol of **2$_{(4)}$**. The yield of **2$_{(6)}$** was 22 %.

3$_{(4)}$: Quinoline methiodide (1.36 g, 5.0 mmol) and triethylamine (7.0 mL, 50 mmol) were added to a mixture (3.24 g) of **2$_{(4)}$** and 2-methylbenzothiazolium bromide in dichloromethane (100 mL). The resulting clear solution was stirred at 25 °C for 16 h. The solvent was removed under reduced pressure. Acetone (200 mL) was then added to the residue. The precipitate was filtered and washed with acetone. The residue was dried under reduced pressure and the red residue was washed with distilled water (50 mL). The precipitate was filtered and washed with distilled water. The residue was dried under reduced pressure to give **3$_{(4)}$** as a red powder (654 mg, 1.39 mmol, 28 %): ^{1}H NMR ([D$_6$]DMSO): $\delta = 8.74$ (d, $J = 8.3$ Hz, 1 H), 8.51 (d, $J = 7.3$ Hz, 1 H), 7.94–7.89 (m, 3 H), 7.74–7.70 (m, 1 H), 7.65 (d, $J = 8.3$ Hz, 1 H), 7.55–7.51 (m, 1 H), 7.36–7.32 (m, 1 H), 7.21 (d, $J = 7.3$ Hz, 1 H), 6.83 (s, 1 H), 4.47 (t, $J = 7.1$ Hz, 2 H), 4.07 (s, 3 H), 2.22 (t, $J = 6.6$ Hz, 1 H), 1.77–1.63 ppm (m, 4 H); ^{13}C NMR ([D$_6$]DMSO, 60 °C): δ = 174.6, 158.8, 148.4, 144.5, 139.5, 137.6, 132.7, 127.9, 126.8, 125.5, 124.1, 123.7, 123.6, 122.4, 117.5, 112.6, 107.6, 87.4, 45.6, 42.0, 35.5, 26.2, 22.3 ppm; HRMS (ESI): calcd for $C_{23}H_{23}N_2O_2S$: 391.1480 $[M-Br]^+$; found: 391.1475.

3$_{(3)}$: The compound was synthesized according to the synthetic protocol of **3$_{(4)}$**. Yield = 43 %. ^{1}H NMR ([D$_6$]DMSO): $\delta = 8.85$ (d, $J = 8.3$ Hz, 1 H), 8.59 (d, $J = 7.3$ Hz, 1 H), 8.02–7.93 (m, 3 H), 7.78–7.70 (m, 2 H), 7.61–7.57 (m, 1 H), 7.42–7.38 (m, 1 H), 7.31 (d, $J = 6.8$ Hz, 1 H), 7.04 (s, 1 H), 4.47 (t, $J = 8.1$ Hz, 2 H), 4.13 (s, 3 H), 2.52–2.48 (m, 2 H), 1.99–1.92 ppm (m, 2 H); ^{13}C NMR ([D$_6$]DMSO, 60 °C): δ = 174.3, 158.9, 148.6, 144.5, 139.5, 137.7, 132.7, 127.9, 126.7, 125.6, 124.1, 124.0, 123.7, 122.5, 117.5, 112.5, 107.6, 87.7, 45.6, 42.0, 31.6, 22.4 ppm; HRMS (ESI): calcd for $C_{22}H_{21}N_2O_2S$: 377.1324 $[M-Br]^+$; found: 377.1316.

3$_{(5)}$: The compound was synthesized according to the synthetic protocol of **3$_{(4)}$**. Yield = 26 %. ^{1}H NMR ([D$_6$]DMSO): $\delta = 8.70$ (d, $J = 8.3$ Hz, 1 H), 8.61 (d, $J = 6.8$ Hz, 1 H), 8.05–8.00 (m, 3 H), 7.80–7.73 (m, 2 H), 7.60–7.56 (m, 1 H), 7.41–7.35 (m, 2 H), 6.89 (s, 1 H), 4.59 (t, $J = 7.3$ Hz, 2 H), 4.16 (s, 3 H), 2.19 (t, $J = 7.3$ Hz, 1 H), 1.82–1.75 (m, 2 H), 1.62–1.43 ppm (m, 4 H); ^{13}C NMR ([D$_6$]DMSO, 60 °C): δ = 174.5, 159.0, 148.6, 144.7, 139.7, 137.8, 132.9, 127.9, 126.9, 125.2, 124.2, 123.8, 123.6, 122.6, 117.8, 112.6, 107.7, 87.4, 45.6, 42.1, 36.0, 26.3, 25.9, 24.9 ppm; HRMS (ESI): calcd for $C_{24}H_{25}N_2O_2S$: 405.1637 $[M-Br]^+$; found: 405.1632.

3$_{(6)}$: The compound was synthesized according to the synthetic protocol of **3$_{(4)}$**. Yield = 22 %. ^{1}H NMR ([D$_6$]DMSO): $\delta = 8.72$ (d, $J = 8.3$ Hz, 1 H), 8.62 (d, $J = 6.8$ Hz, 1 H), 8.07–8.01 (m, 3 H), 7.81–7.75 (m, 2 H), 7.62–7.58 (m, 1 H), 7.42–7.38 (m, 2 H), 6.92 (s, 1 H), 4.61 (t, $J = 7.3$ Hz, 2 H), 4.17 (s, 3 H), 2.18 (t, $J = 7.3$ Hz, 1 H), 1.82–1.75 (m, 2 H), 1.51–1.32 ppm (m, 6 H); ^{13}C NMR ([D$_6$]DMSO, 60 °C): δ = 174.0, 159.1, 148.6, 144.7, 139.8, 137.8, 132.9, 127.9, 126.8, 125.0, 124.2, 123.8, 123.6, 122.6, 118.0, 112.7, 107.8, 87.4, 45.5, 42.1, 33.4, 27.9, 26.4, 25.5, 24.1 ppm; HRMS (ESI): calcd for $C_{25}H_{27}N_2O_2S$: 419.1793 $[M-Br]^+$; found: 419.1788.

4$_{(4)}$: *N*-Hydroxysuccinimide (4.6 mg, 40 μmol) and 1-ethyl-3-(3-dimethylaminopropyl)carbodiimide hydrochloride (7.7 mg, 40 μmol) were added to a solution of **3$_{(4)}$** (9.4 mg, 20 μmol) in *N*,*N*-dimethylformamide (DMF; 0.50 mL) and stirred at 25 °C for 16 h. The reaction mixture was used for the next reaction with DNA **8** without purification.

4$_{(3)}$, **4$_{(5)}$**, and **4$_{(6)}$**: The compound was synthesized according to the synthetic protocol of **4$_{(4)}$**.

6: *N*-Hydroxysuccinimide (460 mg, 4.0 mmol) and 1-ethyl-3-(3-dimethylaminopropyl)carbodiimide hydrochloride (767 mg, 4.0 mmol) were added to a solution of (*E*)-5-(2-carboxyvinyl)-2′-deoxyuridine (**5**; 597 mg, 2.0 mmol) in DMF (5.0 mL) and stirred at 25 °C for 3 h. After the addition of acetic acid (0.5 mL), the solution was dropped into the mixture of dichloromethane (100 mL) and water (100 mL) with vigorous stirring. The precipitate was filtered and washed with water. The residue was dried under reduced pressure overnight. The white residue was suspended in acetonitrile (50 mL) and vigorously stirred. Tris(2-aminoethyl)-amine (3.0 mL, 20 mmol) was added to the suspension and was stirred at 25 °C for 10 min. Ethyl trifluoroacetate (4.8 mL, 40 mmol) and triethylamine (5.6 mL, 40 mmol) were added to the suspension and stirred at 25 °C for 16 h. The mixture was concentrated under reduced pressure and purified by silica gel column chromatography (5–10 % methanol/dichloromethane). The solvent of the fraction that contained **6** was removed under reduced pressure. The residue was dissolved in a small amount of acetone. A white powder precipitated from the mixture upon the addition of diethyl ether. The precipitate was filtered and washed with ether and then dried under reduced pressure to give **6** as a white powder (453 mg, 37 %). ^{1}H NMR (CD_3OD): $\delta = 8.35$ (s, 1 H), 7.22 (d, $J = 15.6$ Hz, 1 H), 7.04 (d, $J = 15.6$ Hz, 1 H), 6.26 (t, $J = 6.6$ Hz, 1 H), 4.44–4.41 (m, 1 H), 3.96–3.94 (m, 1 H), 3.84 (dd, $J = 12.2$, 2.9 Hz, 1 H), 3.76 (dd, $J = 12.2$, 3.4 Hz, 1 H), 3.37–3.30 (m, 6 H), 2.72–2.66 (m, 6 H),2.38–2.23 ppm (m, 2 H); ^{13}C NMR (CD_3OD): $\delta = 169.3$, 163.7, 159.1 (q, $J = 36.4$ Hz), 151.2, 143.8, 134.3, 122.0, 117.5 (q, $J = 286$ Hz), 110.9, 89.1, 87.0, 71.9, 62.5, 54.4, 53.9, 41.7, 38.9, 38.7 ppm; HRMS (ESI): calcd for $C_{22}H_{29}F_6N_6O_8$: 619.1951 $[M+H]^+$; found: 619.1943.

7: A solution of **6** (618 mg, 1.0 mmol) and 4,4′-dimethoxytrityl chloride (373 mg, 1.1 mmol) in pyridine (10 mL) was stirred at 25 °C for 16 h. Water (0.5 mL) was added to the reaction mixture and then the mixture was concentrated under reduced pressure. The residue was purified by silica gel column chromatography (2–4 % methanol and 1 % triethylamine in dichloromethane). The fraction containing the product was then concentrated. Saturated aqueous sodium bicarbonate was added to the residue, and then the mixture was extracted with ethyl acetate, washed with brine, and dried under reduced pressure to give the tritylated product as white foam (735 mg, 80 %): ^{1}H NMR (CD_3OD): $\delta = 7.91$(s, 1 H),

7.39–7.11 (m, 9H), 7.02 (d, $J=15.6$ Hz, 1H), 6.93 (d, $J=15.6$ Hz, 1H), 6.80–6.78 (m, 4H), 6.17 (t, $J=6.6$ Hz, 1H), 4.38–4.35 (m, 1H), 4.06–4.04 (m, 1H), 3.68 (s, 6H), 3.32–3.22 (m, 8H), 2.66–2.55 (m, 6H), 2.40 (ddd, $J=13.7$, 5.9, 2.9 Hz, 1H), 2.33–2.26 ppm (m, 1H); ^{13}C NMR (CD_3OD): $\delta=168.9$, 163.7, 160.1, 159.1 (q, $J=36.9$ Hz), 151.0, 146.1, 143.0, 137.0, 136.9, 134.1, 131.24, 131.16, 129.2, 128.9, 128.0, 122.5, 117.5 (q, $J=286.7$ Hz), 114.2, 110.9, 88.1, 87.9, 87.6, 72.6, 65.0, 55.7, 54.2, 53.9, 41.7, 38.9 ppm, 38.6; HRMS (ESI): calcd for $C_{43}H_{47}F_6N_6O_{10}$: 921.3258 $[M+H]^+$; found: 921.3265. Acetonitrile (5.0 mL) and 2-cyanoethyl *N*,*N*,*N*′,*N*′-tetraisopropylphosphordiamidite (191 μL, 0.60 mmol) were added to a mixture of tritylated nucleoside (188 mg, 0.20 mmol) and 1*H*-tetrazole (28 mg, 0.40 mmol) dried in a round-bottom flask. The mixture was stirred at 25 °C for 2 h. After confirmation of the end of the reaction by TLC, the reaction mixture was diluted with a saturated aqueous solution of sodium bicarbonate and extracted with ethyl acetate. The organic phase was washed with brine, dried over anhydrous magnesium sulfate, filtered, and concentrated in vacuo to give **7**. ^{31}P NMR ($CDCl_3$): $\delta=$ 149.686, 149.430; HRMS (ESI): calcd for $C_{52}H_{64}F_6N_8O_{11}P$: 1121.4336 $[M+H]^+$; found: 1121.4342. Compound **7** was used for automated DNA synthesis without further purification.

8: DNA oligomers were synthesized by a conventional phosphoramidite method by using an Applied Biosystems 392 DNA/RNA synthesizer. Commercially available phosphoramidites were used for dA, dG, dC, and dT. The synthesized DNA oligomer was cleaved from the support with 28% aqueous ammonia and deprotected at 55 °C for 4 h followed by incubation at 25 °C for 16 h. After removal of ammonia from the solution under reduced pressure, the DNA was purified by reversed-phase HPLC on a 5-ODS-H column (10×150 mm^2, elution with a solvent mixture of 0.1 M triethylamine acetate (TEAA), pH 7.0, with a linear gradient over 30 min from 5% to 30% acetonitrile at a flow rate of 3.0 mL min^{-1}). For determination of the concentration of each DNA molecule, the purified DNA was fully digested with calf-intestine alkaline phosphatase (50 U/mL), snake-venom phosphodiesterase (0.15 U/mL), and P1 nuclease (50 U/mL) at 25 °C for 16 h. Digested solutions were analyzed by HPLC on a CHEMCOBOND 5-ODS-H column (4.6×150 mm), eluted with a solvent mixture of 0.1 M TEAA, pH 7.0, flow rate of 1.0 mL min^{-1}. The concentration was determined by comparing peak areas with a standard solution containing dA, dC, dG, and dT at a concentration of 0.1 mM. The DNA was also identified by MALDI-TOF mass spectrometry. CGCAAT**8**-TAACGC, calcd for $C_{134}H_{177}N_{52}O_{76}P_{12}$: 4103.8 $[M+H]^+$; found: 4107.0; TTTTTT**8**TTTTTT, calcd for $C_{138}H_{187}N_{30}O_{90}P_{12}$: 4077.8 $[M+H]^+$; found: 4076.9; TGAAGGGCTT**8**TGAACTCTG, calcd for $C_{205}H_{265}N_{77}O_{122}P_{19}$: 6348.2 $[M+H]^+$; found: 6348.7; GCCTCCT**8**CAGCAAATC-C**8**ACCGGCGTG, calcd for $C_{285}H_{376}N_{108}O_{169}P_{27}$: 8855.0 $[M+H]^+$; found: 8854.8; CCTCCCAAG**8**GCTGGGAT**8**AAAGGCGTG, calcd for $C_{289}H_{376}N_{116}O_{168}P_{27}$: 8999.1 $[M+H]^+$; found: 9002.2.

Bis(thiazole orange)-containing DNA $\mathbf{1}_{(n)}$: A solution of *N*-hydroxysuccinimidyl esters of thiazole orange, $\mathbf{4}_{(n)}$ (50 equiv to an active amino group of DNA) in DMF was added to a solution of deprotected DNA in 100 mM sodium carbonate buffer solution (pH 9.0) and incubated at 25 °C for 16 h. The reaction mixture was diluted with water and passed through a 0.45-μm filter. The product was purified by reversed-phase HPLC on a 5-ODS-H column (10×150 mm^2, elution with a solvent mixture of 0.1 M TEAA, pH 7.0, linear gradient over 30 min from 5% to 30% acetonitrile at a flow rate of 3.0 mL min^{-1}). The concentration of the fluorescent DNA was determined by the same method as described in the DNA synthesis. The fluorescent DNA was identified by MALDI-TOF mass spectrometry. **ODN1** ($n=3$), CGCAAT$\mathbf{1}_{(3)}$TAACGC, calcd for $C_{178}H_{213}N_{56}O_{78}P_{12}S_2$: 4820.7 $[M-H]^+$; found: 4818.9; **ODN1** ($n=4$), CGCAAT$\mathbf{1}_{(4)}$TAACGC, calcd for $C_{180}H_{217}N_{56}O_{78}P_{12}S_2$ 4848.8 $[M-H]^+$; found: 4751.4; **ODN1** ($n=5$), CGCAAT$\mathbf{1}_{(5)}$TAACGC, calcd for $C_{182}H_{221}N_{56}O_{78}P_{12}S_2$: 4876.8 $[M-H]^+$; found: 4875.6; **ODN1** ($n=6$), CGCAAT$\mathbf{1}_{(6)}$TAACGC, calcd for $C_{184}H_{225}N_{56}O_{78}P_{12}S_2$: 4904.9 $[M-H]^+$; found: 4903.6; **ODN2**, TTTTTT$\mathbf{1}_{(4)}$TTTTTT, calcd for $C_{184}H_{227}N_{34}O_{92}P_{12}S_2$: 4822.8 $[M-H]^+$; found: 4821.4; **ODN3**, TGAAGGGCTT$\mathbf{1}_{(4)}$TGAACTCTG, calcd for $C_{251}H_{305}N_{81}O_{124}P_{19}S_2$: 7093.2 $[M-H]^+$; found: 7092.3; **ODN(anti4.5S)**, GCCTCCT$\mathbf{1}_{(4)}$CAGCAAATCC$\mathbf{1}_{(4)}$ACCGGCGTG, calcd for $C_{377}H_{456}N_{116}O_{173}P_{27}S_4$: 10344.9 $[M-3H]^+$; found: 10342.7; **ODN(antiB1)**,CCTCCCAAG$\mathbf{1}_{(4)}$GCTGGGAT$\mathbf{1}_{(4)}$AAAGGCGTG, calcd for $C_{381}H_{456}N_{124}O_{172}P_{27}S_4$: 10489.0 $[M-3H]^+$; found: 10489.8. The synthetic protocol of $\mathbf{9}_{(4)}$-containing DNA, **ODN4** and **ODN5**, and their mass data are described in the Supporting Information.

Absorption, Fluorescence, and CD Measurements

Absorption, fluorescence, and CD spectra of the fluorescent probes (2.5 μM, single strand or duplex concentration) were measured in 50 mM sodium phosphate buffer solution (pH 7.0) containing 100 mM sodium chloride by using a cell with a 1-cm path length. The excitation and emission bandwidths were 1.5 nm.

Melting-Temperature Measurements

The T_m values of duplexes (2.5 μM, final duplex concentration) were measured in 50 mM sodium phosphate buffers (pH 7.0) containing 100 mM sodium chloride. The absorbance of the samples was monitored at 260 nm from 10 °C to 90 °C with a heating rate of 0.5 °C min^{-1}. From these profiles, first derivatives were calculated to determine the value of T_m.

Dot-Blot Analysis

We prepared two DNA fragments: a DNA duplex containing a 4.5S RNA sequence, 5′-d(GCCGGTAGTGGTGGCGCACGCCGGTAG-GATTTGCTGAAGGAGGCAGAGGCAGGAGGATCACGAGTTC-GAGGCCAGCCTGGGCTACACATTTTTTT)-3’ and its complementary DNA; and a DNA duplex containing a B1 RNA, 5′-d(GCCGGGCATGGTGGCGCACGCCTTTAATCCCAGCACTTGG-GAGGCAGAGGCAGGCGGATTTCTGAGTTCGAGGCCAGCCTG-GTCTACAGAGTGAG)-3’ and its complementary DNA. The DNA duplexes were denatured in 0.5 M sodium hydroxide and 1 M sodium chloride. Aliquots of DNA were dotted onto a positively charged nylon membrane (Roche). After wetting the membrane sheet with 50 mM sodium phosphate and 100 mM sodium chloride, the sheet was incubated in 50 mM sodium phosphate, 100 mM sodium chloride, and 100 μg mL^{-1} salmon sperm DNA at 50 °C for 30 min. After the addition of a solution of probe (150 pmol of **ODN(anti4.5S)** or **ODN(antiB1)**) in 50 mM sodium phosphate and 100 mM sodium chloride, the sheet was incubated at 50 °C for 1 h. The hybridization buffer solution was removed after being cooled to room temperature, and then the fluorescence from the membrane sheet was observed in a fresh sodium phosphate buffer solution by using a VersaDoc imaging system (BioRad). The light from a UV transilluminator Model-2270 (Wakenyaku) through a UV/blue converter plate (UVP) was used as the excitation light.

Acknowledgements

We thank Dr. Shinichi Nakagawa (Frontier Research System, RIKEN) for technical instruction in dot blotting. We also thank Dr. Takemichi Nakamura (Molecular Characterization Team, RIKEN) for the ESI mass spectrometry and Dr. Takehiro Suzuki (Biomolecular Characterization Team, RIKEN) for the MALDI-TOF mass spectrometry. This research was supported by the Industrial Technology Research Grant Program in 2006 from the New Energy and Industrial Technology Development Organization (NEDO) of Japan.

[1] a) V. Bernard, *Molecular Fluorescence*, Wiley-VCH, Weinheim, Germany, **2002**; b) G. Loeber, *J. Lumin.* **1981**, *22*, 221–265; c) R. M. Williams, W. R. Zipfel, W. W. Webb, *Curr. Opin. Chem. Biol.* **2001**, *5*, 603–608; d) H. Ihmels, D. Otto, *Top. Curr. Chem.* **2005**, *258*, 161–204; e) A. Okamoto, Y. Saito, I. Saito, *J. Photochem. Photobiol. C* **2005**, *6*, 108–122; f) K. M. Marks, G. P. Nolan, *Nat. Methods* **2006**, *3*, 591–596; g) N. Johnsson, K. Johnsson, *ACS Chem. Biol.* **2007**, *2*, 31–38.

[2] a) I. Aoki, H. Kawabata, K. Nakashima, S. Shinkai, *J. Chem. Soc. Chem. Commun.* **1991**, 1771–1773; b) S. Nishizawa, Y. Kato, N. Ter-

amae, *J. Am. Chem. Soc.* **1999**, *121*, 9463–9464; c) A. Okamoto, T. Ichiba, I. Saito, *J. Am. Chem. Soc.* **2004**, *126*, 8364–8365; d) H. N. Lee, Z. Xu, S. K. Kim, K. M. K. Swamy, Y. Kim, S.-J. Kim, J. Yoon, *J. Am. Chem. Soc.* **2007**, *129*, 3828–3829.

[3] a) G. Weber, F. J. Farris, *Biochemistry* **1979**, *18*, 3075–3078; b) G. Grynkiewicz, M. Poenie, R. Y. Tsien, *J. Biol. Chem.* **1985**, *260*, 3440–3450; c) R. B. Macgregor, G. Weber, *Nature* **1986**, *319*, 70–73; d) D. W. Pierce, S. G. Boxer, *J. Phys. Chem.* **1992**, *96*, 5560–5566; e) M. M. Martin, P. Plaza, Y. H. Meyer, F. Badaoui, J. Bourson, J. P. Lefèvre, B. Valeur, *J. Phys. Chem.* **1996**, *100*, 6879–6888; f) B. E. Cohen, T. B. McAnaney, E. S. Park, Y. N. Jan, S. G. Boxer, L. Y. Jan, *Science* **2002**, *296*, 1700–1703; g) A. Okamoto, K. Tainaka, K.-i. Nishiza, I. Saito, *J. Am. Chem. Soc.* **2005**, *127*, 13128–13129; h) A. Okamoto, K. Tainaka, T. Unzai, I. Saito, *Tetrahedron* **2007**, *63*, 3465–3470; i) K. Tainaka, K. Tanaka, S. Ikeda, K.-i. Nishiza, T. Unzai, Y. Fujiwara, I. Saito, A. Okamoto, *J. Am. Chem. Soc.* **2007**, *129*, 4776–4784.

[4] a) F. Fages, J. P. Desvergne, H. Bouas-Laurent, P. Marsau, J. M. Lehn, F. Kotzyba-Hibert, A. M. Albrecht-Gary, M. Al-Joubbeh, *J. Am. Chem. Soc.* **1989**, *111*, 8672–8680; b) R. A. Bissell, A. P. de Silva, H. Q. N. Gunaratne, P. L. M. Lynch, G. E. M. Maguire, C. P. McCoy, K. R. A. S. Sandanayake, *Top. Curr. Chem.* **1993**, *168*, 223–264; c) T. D. James, K. R. A. S. Sandanayake, R. Iguchi, S. Shinkai, *J. Am. Chem. Soc.* **1995**, *117*, 8982–8987; d) R. Bergonzi, L. Fabbrizzi, M. Lichelli, C. Mangano, *Coord. Chem. Rev.* **1998**, *170*, 31–46; e) G. K. Walkup, S. C. Burdette, S. L. Lippard, R. Y. Tsien, *J. Am. Chem. Soc.* **2000**, *122*, 5644–5645; f) T. Miura, Y. Urano, K. Tanaka, T. Nagano, K. Ohkubo, S. Fukuzumi, *J. Am. Chem. Soc.* **2003**, *125*, 8666–8671; g) Y. Urano, M. Kamiya, K. Kanda, T. Ueno, K. Hirose, T. Nagano, *J. Am. Chem. Soc.* **2005**, *127*, 4888–4894.

[5] a) P. Wu, K. G. Rice, L. Brand, Y. C. Lee, *Proc. Natl. Acad. Sci. USA* **1991**, *88*, 9355–9359; b) J.-L. Mergny, A. S. Boutorine, T. Garestier, F. Belloc, M. Rougée, N. V. Bulychev, A. A. Koshkin, J. Bourson, A. V. Lebedev, B. Valeur, N. T. Thuong, C. Hélène, *Nucleic Acids Res.* **1994**, *22*, 920–928; c) P. Wu, L. Brand, *Anal. Biochem.* **1994**, *218*, 1–13; d) A. Hillisch, M. Lorenz, S. Diekmann, *Curr. Opin. Struct. Biol.* **2001**, *11*, 201–207; e) D. Klostermeier, D. P. Millar, *Biopolymers* **2002**, *67*, 159–179.

[6] a) S. Tyagi, F. R. Kramer, *Nat. Biotechnol.* **1996**, *14*, 303–308; b) S. Tyagi, D. P. Btaru, F. R. Kramer, *Nat. Biotechnol.* **1998**, *16*, 49–53; c) A. S. Piatek, S. Tyagi, A. C. Pol, A. Telenti, L. P. Miller, F. R. Kramer, D. Alland, *Nat. Biotechnol.* **1998**, *16*, 359–363; d) X. Fang, J. J. Li, J. Perlette, W. Tan, K. Wang, *Anal. Chem.* **2000**, *72*, 747 A-753 A; e) N. E. Broude, *Trends Biotechnol.* **2002**, *20*, 249–256; f) A. Okamoto, K. Tanabe, T. Inasaki, I. Saito, *Angew. Chem.* **2003**, *115*, 2606–2608; *Angew. Chem. Int. Ed.* **2003**, *42*, 2502–2504; g) W. Tan, K. Wang, T. J. Drake, *Curr. Opin. Chem. Biol.* **2004**, *8*, 547–553.

[7] a) L. G. Lee, C.-H. Chen, L. A. Chiu, *Cytometry* **1986**, *7*, 508–517; b) J. Nygren, N. Svanvik, M. Kubista, *Biopolymers* **1998**, *46*, 39–51; c) S. Ikeda, A. Okamoto, *Photochem. Photobiol. Sci.* **2007**, *6*, 1197–1201.

[8] H. S. Rye, S. Yue, D. E. Wemmer, M. A. Quesada, R. P. Haugland, R. A. Mathies, A. N. Glazer, *Nucleic Acids Res.* **1992**, *20*, 2803–2812.

[9] J. P. Jacobsen, J. B. Pedersen, L. F. Hansen, D. E. Wemmer, *Nucleic Acids Res.* **1995**, *23*, 753–760.

[10] a) D. Hanafi-Bagby, P. A. E. Piunno, C. C. Wust, U. J. Krull, *Anal. Chim. Acta* **2000**, *411*, 19–30; b) X. Wang, U. J. Krull, *Anal. Chim. Acta* **2002**, *470*, 57–70; c) X. Wang, U. J. Krull, *Bioorg. Med. Chem. Lett.* **2005**, *15*, 1725–1729; d) U. Asseline, M. Chassignol, Y. Aubert, V. Roig, *Org. Biomol. Chem.* **2006**, *4*, 1949–1957; e) R. Lartia, U. Asseline, *Chem. Eur. J.* **2006**, *12*, 2270–2281.

[11] The first example of a fluorogenic cyanine-DNA conjugate and its use for RNA detection: T. Ishigro, J. Saitoh, H. Yawata, M. Otsuka, T. Inoue, Y. Sugiura, *Nucleic Acids Res.* **1996**, *24*, 4992–4997.

[12] a) N. Svanvik, J. Nygren, G. Westman, M. Kubista, *J. Am. Chem. Soc.* **2001**, *123*, 803–809; b) O. Köhler, D. V. Jarikote, O. Seitz, *Chem. Commun.* **2004**, 2674–2675; c) D. V. Jarikote, O. Köhler, E. Socher, O. Seitz, *Eur. J. Org. Chem.* **2005**, 3187–3195; d) V. L. Marin, B. A. Armitage, *Biochemistry* **2006**, *45*, 1745–1754.

[13] a) R. F. Khairutdinov, N. Serpone, *J. Phys. Chem. B* **1997**, *101*, 2602–2610; b) L. D. Simon, K. H. Abramo, J. K. Sell, L. B. McGown, *Biospectrosc.* **1998**, *4*, 17–25; c) G. Cosa, K.-S. Focsaneanu, J. R. N. McLean, J. P. McNamee, J. C. Scaiano, *Photochem. Photobiol.* **2001**, *73*, 585–599; d) T. Sagawa, H. Tobata, H. Ihara, *Chem. Commun.* **2004**, 2–4; e) A. Fürstenberg, M. D. Julliard, T. G. Deligeorgiev, N. I. Gadjev, A. A. Vasilev, E. Vauthey, *J. Am. Chem. Soc.* **2006**, *128*, 7661–7669.

[14] a) W. West, S. Pearce, *J. Phys. Chem.* **1965**, *69*, 1894–1903; b) V. Czikkely, H. D. Forsterling, H. Kuhn, *Chem. Phys. Lett.* **1970**, *6*, 207–210; c) W. J. Harrison, D. L. Mateer, G.-J. Tiddy, Jr., *J. Phys. Chem.* **1996**, *100*, 2310–2321; d) S. Zeena, K. G. Thomas, *J. Am. Chem. Soc.* **2001**, *123*, 7859–7865; e) K. C. Hannah, B. A. Armitage, *Acc. Chem. Res.* **2004**, *37*, 845–853; f) U. Rösch, S. Yao, R. Wortmann, F. Würthner, *Angew. Chem.* **2006**, *118*, 7184–7188; *Angew. Chem. Int. Ed.* **2006**, *45*, 7026–7030.

[15] a) S. C. Benson, P. Singh, A. N. Glazer, *Nucleic Acids Res.* **1993**, *21*, 5727–5735; b) N. Svanvik, G. Westman, D. Wang, M. Kubista, *Anal. Biochem.* **2000**, *281*, 26–35; c) E. Privat, U. Asseline, *Bioconjugate Chem.* **2001**, *12*, 757–769.

[16] M. Ashwell, A. S. Jones, A. Kumar, J. R. Sayers, R. T. Walker, T. Sakuma, E. de Clercq, *Tetrahedron* **1987**, *43*, 4601–4608.

[17] M. Kasha, *Radiat. Res.* **1963**, *20*, 55–70.

[18] a) A. Larsson, C. Carlsson, M. Jonsson, B. Albinsson, *J. Am. Chem. Soc.* **1994**, *116*, 8459–8465; b) H. S. Rye, A. N. Glazer, *Nucleic Acids Res.* **1995**, *23*, 1215–1222; c) J. T. Petty, J. A. Bordelon, M. E. Robertson, *J. Phys. Chem. B* **2000**, *104*, 7221–7227; d) D. V. Jarikote, N. Krebs, S. Tannert, B. Röder, O. Seitz, *Chem. Eur. J.* **2007**, *13*, 300–310.

[19] C. Carlsson, A. Larsson, M. Jonsson, B. Albinsson, B. Norden, *J. Phys. Chem.* **1994**, *98*, 10313–10321.

[20] a) S. Adeniyi-Jones, M. Zasloff, *Nature* **1985**, *317*, 81–84; b) R. J. Maraia, *Nucleic Acids Res.* **1991**, *19*, 5695–5702; c) N. S. Vassetzky, O. A. Ten, D. A. Kramerov, *Gene* **2003**, *319*, 149–160.

[21] a) F. Harada, N. Kato, *Nucleic Acids Res.* **1980**, *8*, 1273–1285; b) S. R. Haynes, T. P. Toomey, L. Leinwand, W. R. Jelinek, *Mol. Cell. Biol.* **1981**, *1*, 573–583; c) L. O. Schoeniger, W. R. Jelinek, *Mol. Cell. Biol.* **1986**, *6*, 1508–1519; d) F. Harada, Y. Takeuchi, N. Kato, *Nucleic Acids Res.* **1986**, *14*, 1629–1642; e) F. Bovia, K. Strub, *J. Cell Sci.* **1986**, *109*, 2601–2608; f) R. Kraft, L. Kadyk, L. A. Leinwand, *Genomics* **1992**, *12*, 555–566.

Received: January 17, 2008
Published online: April 30, 2008

